Accepted Manuscript

Phage display technique identifies the interaction of SARS coronavirus ORF6 protein with nuclear pore complex interacting protein NPIPB3 in modulating Type I interferon antagonism

Su-Hua Huang, Tzu-Ying Lee, Ying-Ju Lin, Lei Wan, Chih-Ho Lai, Cheng-Wen Lin, PhD, Professor

PII: S1684-1182(15)00805-1

DOI: 10.1016/j.jmii.2015.07.002

Reference: JMII 655

To appear in: *Journal of Microbiology, Immunology and Infection*

Received Date: 27 January 2015

Revised Date: 9 June 2015

Accepted Date: 6 July 2015

Please cite this article as: Huang S-H, Lee T-Y, Lin Y-J, Wan L, Lai C-H, Lin C-W, Phage display technique identifies the interaction of SARS coronavirus ORF6 protein with nuclear pore complex interacting protein NPIPB3 in modulating Type I interferon antagonism, *Journal of Microbiology, Immunology and Infection* (2015), doi: 10.1016/j.jmii.2015.07.002.

June 8, 2015

Phage display technique identifies the interaction of SARS coronavirus ORF6 protein with nuclear pore complex interacting protein NPIPB3 in modulating Type I interferon antagonism

Su-Hua Huang[1] Tzu-Ying Lee[2] Ying-Ju Lin[3] Lei Wan[3]
Chih-Ho Lai[4] Cheng-Wen Lin[1,2*]

[1]Department of Biotechnology, Asia University, Wufeng, Taichung, Taiwan.

[2]Department of Medical Laboratory Science and Biotechnology, China Medical University, Taichung, Taiwan.

[3]Department of Medical Genetics and Medical Research, China Medical University Hospital, Taichung 404, Taiwan

[4]School of Medicine, Department of Microbiology, China Medical University, Taichung 404, Taiwan

Short title: Interaction of SARS-CoV ORF6 and SMG-1

*Corresponding author.

Mailing address: Cheng-Wen Lin, PhD, Professor. Department of Medical Laboratory Science and Biotechnology, China Medical University, No. 91, Hsueh-Shih Road, Taichung, Taiwan 40402, R.O.C.

Phone: +886-4-2205-3366 ext 7210

Fax: +886-4-22057414.

Email: cwlin@mail.cmu.edu.tw

Abstract

Background: Severe acute respiratory syndrome coronavirus (SARS-CoV) proteins including ORF6 inhibit Type I interferon (IFN) signaling.

Methods: This study identified SARS-CoV ORF6-interacting proteins using the phage displayed human lung cDNA libraries, and examined the association of ORF6-host factor interaction with Type I IFN antagonism. After fifth round of biopanning with *E. coli*-synthesized ORF6-His tagged protein, relative binding affinity of phage clones to ORF6 were determined using direct ELISA.

Results: The highest affinity clone to ORF6 displayed C-terminal domain of NPIPB3 (nuclear pore complex interacting protein family, member B3; also named as PI-3-kinase-related kinase SMG-1 isoform 1 homolog). Co-immunoprecipitation assay demonstrated direct binding of ORF6 to C-terminal domain of NPIPB3 *in vitro*. Confocal imaging revealed a close co-localization of SARS-CoV ORF6 protein with NPIPB3 in human promonocytes. Dual luciferase reporter assay showed that C-terminal domain of NPIPB3 attenuating antagonistic activity of SARS-CoV ORF6 on IFNβ-induced ISRE-responsive firefly luciferase activity. In addition, confocal imaging and Western blotting assays revealed that the increases of STAT-1 nuclear translocation and phophorylation were found in the transfected cells expressing both genes of ORF6 and NPIPB3, but not in the ORF6-expressing cells in response to IFNβ.

Conclusion: Overexpression of NPIPB3 restored the INFβ responses in SARS-CoV ORF6 expressing cells, indicating the interaction of SARS CoV ORF6 and NPIPB3 reducing Type I IFN antagonism by SARS-CoV ORF6.

Keywords: SARS-CoV, ORF6, IFN antagonism, phage display, NPIPB3

Introduction

Pandemic outbreak of severe acute respiratory syndrome coronavirus (SARS-CoV) arises from the Guangdong Province of China in November 2002, affecting over 8500 cases worldwide.[1,2] Middle East respiratory syndrome coronavirus (MERS-CoV) emerges from the Arabian Peninsula in 2012, globally identified in 941 laboratory-confirmed cases with 347 related deaths until 26 December 2014 notified by WHO (World Health Organization, http://www.who.int/csr/don/26-december- 2014-mers/en/). CoV genome is a single-stranded, positive-sense RNA of ~30 kb, contains 14 potential open reading frames (ORFs), and encodes replicase (ORF1a and ORF1ab), structural proteins (spike, nucleocapsid, membrane and envelope), and accessory proteins (ORF 3a, ORF 3b, ORF6, ORF 7a, ORF 7b, ORF 8a, ORF 8b and ORF 9b).[3] These accessory proteins could be dispensable for virus replication, but might have a specific function in viral infection. ORF3 and ORF 7a proteins activate JNK and NF-κB signaling, up-regulate IL-8 and RANTES, and modulate apoptosis and cell cycle.[4,5] ORF 3b and ORF6 proteins modulate the host innate immune response, including inhibition of Type I IFN production and signaling.[4,5]

SARS-CoV ORF6 protein localizes in the membrane of endoplasmic reticulum (ER) and Golgi apparatus in infected cells[6]; ORF6 ever-expression triggers the ER stress in transfected cells.[7] ORF6 protein is dispensable for viral replication *in vitro* and *in vivo*[8], but associates with viral escape from innate immune, particularly inhibition of Type I interferon (IFN) production and signaling pathways.[7,9] ORF6 protein interacts with the C-terminus of karyopherin alpha 2, leading to impeding the nuclear import of phosphorylated STAT1 in response to IFNβ. Thus, SARS-CoV

ORF6 protein is an antagonist of Type I IFNs. In this study, we identified cellular ORF6-interacting factors using phage display human lung cDNA library, further examining the association of SARS-CoV ORF6 and host factors in Type I IFN antagonism. The C-terminus of nuclear pore complex interacting protein NPIPB3 (Gene ID: 23117), also known as phosphatidylinositol (PI)-3-kinase-related kinase SMG-1 isoform 1 homolog, displayed on phage surface showed the highest binding affinity to recombinant ORF6 protein. The interaction of ORF6 and NPIPB3 was analyzed using co-immunoprecipitation *in vitro* and co-localization in cells. Effect of NPIPB3 over-expression on Type I IFN antagonism of ORF6 was determined using dual-luciferase reporter assay system, and STAT1 phosphorylation and nuclear translocation.

Materials and methods

Construction and expression of recombinant ORF6 protein in E. coli and human promocyte HL-CZ cells

For generating bacterial and mammalian expression of recombinant ORF6 protein, SARS-CoV ORF6 gene of the SARS-CoV TW1 strain genome (GenBank Accession No. AY291451), was amplified by RT-PCR from genome RNA template and cloned into the pTriEx™-4 Neo vector for the production of recombinant ORF6 protein fused with an N-terminal His-Tag. The primers included 5′ATCGGAATTCTATGTTTCATCCGTT-3′ and 5′-ATCGGCGGCCGCTGGATAATC TAACTC-3′. Forward primer contained an *Eco*RI restriction site; reverse primer included a *Not*I restriction site. Amplified RT-PCR product was cloned into pTriEx™-4 Neo vector (Novagen), resulting construct named pTriEx-ORF6. For the production of *E. coli*-synthesized ORF6 protein, pTriEx-ORF6 was transformed into *E.*

coli BL21 (DE3) cells. The induction expression and purification of *E. coli*-synthesized ORF6 protein were performed as described in our prior reports.[10,11] Finally, recombinant ORF6 protein was purified using immobilized-metal affinity chromatography as described in our prior study[12], and then analyzed by Western blotting with anti-His tag monoclonal antibody and alkaline phosphatase-conjugated goat anti-mouse IgG antibodies. The immunoreactive band was developed with TNBT/BCIP (Invitrogen).

Biopanning of a phage display human cDNA library with SARS-CoV ORF6 protein

For identifying ORF6-interacting proteins, a human lung cDNA library (Novagen) was used to screen high-affinity phage clones to recombinant ORF6, as previously described.[10,11] Briefly, biopanning of the phage display lung cDNA library was performed using ORF6-coated microplates. After five rounds of biopanning, ORF6-interacting phage clones were eluted with the soluble ORF6 protein. ORF6-interacting phage clone was randomly picked up from individual plaques, amplified in *E. coli*, and then used for determining the binding affinity to recombinant ORF6 protein using direct ELISA. The nucleotide sequences of ORF6-interacting proteins displayed on the high affinity phage clones were directly sequenced; their deduced amino acid sequences were analyzed using the BLAST search (http://www.ncbi.nlm.nih.gov/BLAST/).

Co-immunoprecipitation and co-localization assays

The nucleotide sequences of the C-terminus (amino acid residues 936-1050) of NPIPB3 (Accession number Q92617) fused with the coat protein of ORF6-interacting phage clone 40 was amplified using PCR, and then cloned into

bacterial expression vector pET32a for co-immunoprecipitation *in vitro* and mammalian expression vector pDsRed1-C (BD Biosciences Clontech) for co-localization assay. Two primer pairs were 5′-ATCGGATATCTCAAGCGAGGCAGAAAAA-3′ and 5′-ATCGGA ATTCGCTCAACCTCCGCCTCTT-3′ for pET32a cloning, as well as 5′-ATCGATGAAGCTTATTCAAGCGAGGCAGAA-3′ and 5′-ATCGATGGGATC CGCTCAACCTCCGCCTCTT-3′ for pDsRed1-C cloning, respectively. For co-immunoprecipitation assays, *E. coli* BL21 (DE3) cells were transformed with pET32a-NPIPB3; *E. coli*-synthesized C-terminal domain of NPIPB3 protein was induced and purified using immobilized-metal affinity chromatography as described in our prior studies.[10-12] Recombinant C-terminal domain of NPIPB3 with a thioredoxin (Trx) at the N-terminus and a His-tag at the C-terminus was mixed with recombinant ORF6 protein with an N-terminal His-Tag; the mixture was incubated with the anti-Trx mAb in cool room overnight, followed by addition of protein A-Sepharose beads for an additional 2-h. After centrifugation, the immunoprecipitate was analyzed using Western blotting with the anti-His tag mAb for a 1-h incubation period. The immune-reactive complexes were detected using horseradish peroxidase-conjugated goat anti-mouse IgG antibodies, and then developed using enhanced chemiluminescence reaction (Amersham Pharmacia Biotech). For co-localization assays, pTriEx-ORF6 plus pDsRed1-C (BD Biosciences Clontech), pTriEx-ORF6 plus pDsRed-NPIPB3, pTriEx plus pDsRed1-C, or pTriEx plus pDsRed-NPIPB3 were co-transfected into HL-CZ cells (human promonocyte cell line) with GenePorter reagent. Transfected cells were generated, fixed, and stained with primary antibodies against His-tag, followed by FITC-conjugated anti--mouse IgG antibodies, as described in our

prior studies.[13,14] Confocal image of stained cells was taken using Leica TCS SP2 AOBS laser-scanning microscopy (Leica Microsystems, Heidelberg GmbH, Germany). In cells, red fluorescence indicated DsRed-NPIPB3 fusion protein, while green fluorescence was ORF6-His tag fusion protein. The colocalization of DsRed-NPIPB3 and ORF6 appeared as orange to yellow.

Dual-luciferase reporter assay of ISRE promoter

HL-CZ cells expressing single and both of ORF6 and NPIPB3, described above, were further co-transfected with pISRE-Luc *cis*-reporter (Stratagene) and control reporter pRluc-C1, treated with IFNβ (Hoffmann-La Roche) for 4 h, and then harvested. The activity of experimental firefly luciferase and control renilla luciferase in lysate was measured using dual Luciferase Reporter Assay System (Promega) and TROPIX TR-717 Luminometer (Applied Biosystems) described by Lin *et al.*[11]

Subcellular localization assays of STAT1

HL-CZ cells expressing single and both of ORF6 and NPIPB3, described above, were treated with IFNβ (Hoffmann-La Roche) for 1 h, and then harvested. Cells were fixed by cold methanol, incubated with anti-STAT1 mAb for 2 h, followed by FITC-conjugated anti-mouse IgG antibodies for additional 2 h. Finally, cells were stained with 4', 6-diamidino-2-phenylindole (DAPI) for 10 min. Photographs of cells were taken by immunofluorescent microscopy.

Western blotting of STAT1 phosphorylation

For testing the effect of ORF6 and NPIPB3 interaction on IFN-stimulated STAT1 activation, lysate from cells expressing single and both of ORF6 and NPIPB3 treated with IFNβ for 15 and 30 min was performed using Western blotting with anti-phosphotyrosine STAT1 (Tyr701), and anti-β actin mAb (Cell Signaling Technology). The immune-reactive bands were probed by horseradish peroxidase-conjugated goat anti-mouse IgG antibodies, and then developed using enhanced chemiluminescence reagents.

Statistical analysis

Three independent experiments in each independent result were performed; all data were represented as mean ± standard deviation (S.D.) and statistically analyzed using SPSS program (version 10.1, SPSS Inc., IL) via one-way ANOVA analysis by Scheffe test.

Results

Selection of SARS-CoV ORF6-interacting host facts using phage display library

SARS-CoV ORF6, cloned into pTriEx-4 vector, was synthesized as a 17.5kDa fusion protein with an N-terminal His-Tag in *E. coli* that was purified using immobilized-metal affinity chromatography (Fig. 1). Recombinant ORF6 protein was used for the selection of its interacting cellular factors with phage displayed a human lung cDNA library. After fifth round of biopanning, ORF6-specific binding phage clones eluted were selected from single phage plaques, amplified in *E. coli* for determining relative ORF6-binding affinities.

Each phage clone was performed by direct binding ELISA assay in ORF6-coated wells (Fig. 2). Phage clones No. 16, 26, and 40 with higher binding affinity to ORF6 were quantitated using plaque assays (P <0.01), subsequently measured the binding specificity (Fig. 3). Phage clones No. 16, 26, and 40 bound to recombinant ORF6 protein in a dose-dependent manner. Among three phage clones, clone No. 40 at a titer of 10^7 phages showed the highest affinity to ORF6 protein (P < 0.001). ORF6-interacting protein-encoding sequences fused in-frame with protein III gene of phage clones No. 16, 26, and 40 were sequenced. BLAST alignment search of the nucleotide sequences indicated ORF6-interacting protein display phage clones No. 16, 26, and 40 were identified as CCNL1 (cyclin L1), RBMXL2 (RNA binding motif protein, X-linked-like 2), and NPIPB3 (nuclear pore complex interacting protein family, member B3), respectively. Because NPIPB3 displayed on phage clone 40 had the highest binding affinity to ORF6 protein (Fig. 3), the interaction between ORF6 and NPIPB3 was further evaluated.

In vitro and in vivo interaction of ORF6 with NPIPB3

To test *in vitro* and *in vivo* interaction between ORF6 and NPIPB3, the C-terminus (amino acid residues 936-1050) of NPIPB3 was cloned into bacterial expression vector pET32a for *in vitro* co-immunoprecipitation and mammalian expression vector pDsRed1-C for *in vivo* co-localization assay (Figs. 4 and 5). In co-immunoprecipitation assay, ORF6-His tag protein reacted with Trx-NPIPB3-His tag fusion protein for 4 hours in cool room, and then the protein complex were co-immunoprecipitated using anti-Trx antibodies and protein A-Sepharose beads. Co-immunoprecipitates were analyzed Western blotting with the anti-His tag antibodies (Fig. 4). Western blotting analysis of immunoprecipitates revealed that

ORF protein bound to Trx-NPIPB3-His tag fusion protein, but not Trx protein (Fig. 4, lane 3 vs. lane 1). In co-localization assay, single and both of DsRed-NPIPB3 and ORF6-His tag protein were expressed in human promonocyte HL-CZ cells. After immunofluorescence staining with anti-His tag and FITC-conjugated anti-mouse IgG antibodies, confocal microscopy revealed a very close co-localization of DsRed-NPIPB3 and ORF6-His tag protein appearing as orange to yellow fluorescent light (Fig. 5P), but no colocalization between DsRed and ORF6-His tag protein, or DsRed-NPIPB3 and His tag protein (Figs. 5D, 5H and 5L). The results demonstrated SARS-CoV ORF6 directly interacting with the C-terminus of NPIPB3 *in vitro* and *in vivo*.

Attenuation effect of NPIPB3 overexpression on Type I IFN antagonistic activity of SARS-CoV ORF6

To determine the role of NPIPB3 in Type I IFN antagonism of SRAS-CoV ORF6, IFN-β induced responses of transfected cells with single or both of pDsRed-NPIPB3 and pTriEx-ORF6 were explored using ISRE luciferase reporter, STAT1 subcellular localization, and Western blotting assays (Figs. 6-8). Transient overexpression of NPIPB3 C-terminus improved 2.5-fold increase of the ISRE promoter activity in ORF6-expressing cells in response to IFN-β (Fig. 6; $P<0.001$). To examine subcellular location of STAT1, confocal imaging analysis indicated overexpression of NPIPB3 C-terminus did not change subcellular localization of STAT1 in vector control and ORF6-expressing cells (Figs. 7A(4)-(6) and 7A(10)-(12)). IFNβ treatment stimulated STAT1 nuclear translocation in vector control cells (Figs. 7B(1)-(3)), but not in ORF6-expressing cells (Figs. 7B(7)-(9)). However, NPIPB3 C-terminus overexpression significantly enhanced IFNβ-induced

STAT1 nuclear translocation in ORF6-expressing cells (Figs. 7B(10)-(12)). In addition, Western blotting indicated NPIPB3 C-terminus overexpression enhancing IFNβ-induced STAT1 phosphorylation at Tyr701 in ORF6-expressing cells (Fig. 8). Results demonstrated NPIPB3 C-terminus overexpression reducing Type I IFN antagonism of SARS-CoV ORF6 via activating STAT1-mediated signal pathways.

Discussion

The study demonstrated Type I IFN antagonism of SARS-CoV ORF6 through the inhibition of IFNβ-induced STAT1 phosphorylation and nuclear translocation in human promonocytes (Figs. 6-8), as consistent with a previous report in that ORF6 blocked STAT1 nuclear translocation in response to Type I IFNs through disrupting import complex formation by binding with karyopherin alpha 2.[6] C-terminal hydrophilic domain of ORF6 interacted with cellular karyopherins, but N-terminal lipophilic part of ORF6 was also required for retaining cellular karyopherins at the ER/Golgi membrane, leading to impede nuclear import.[15] Besides STAT1, SARS-CoV ORF6 affected on the activity of karyopherin-dependent transcription factors, including VDR, CREB1, SMAD4, p53, EpasI, and Oct3/4.[16] Therefore, ORF6 plays the vital role in innate antiviral responses.

Biopanning of phage displayed human lung cDNA libraries identified the binding interaction of ORF6 with its interacting host factors, including CCNL1 (cyclin L1), RBMXL2 (RNA binding motif protein, X-linked-like 2), and NPIPB3 (nuclear pore complex interacting protein family, member B3) (Figs. 2 and 3). CCNL1 displayed on phage clone No. 16, containing an arginine and serine-rich domain and a cyclin domain, was required for spliceosome assembly and regulated splicing.[17,18] RBMXL2 displayed on phage clone No. 26 was one of heterogeneous

nuclear ribonucleoproteins, suggested as a germ cell-specific splicing regulator.[19] ORF6-interacting phage clone No. 40 displayed the C-terminal domain of NPIPB3 (Figs. 2 and 3). NPIPB3 had many alternative names such as nuclear pore complex-interacting protein-like 3, protein pps22-1, KIAA0220-like protein, nuclear pore complex-interacting protein B type, and PI-3-kinase-related kinase SMG-1 isoform 1 homolog.[20] NPIPB3 containing a transmembrane region at the N-terminus, was recognized as a membrane protein and served as a RNA splicing factor. NPIPB3 was up-regulated in epithelial Caco-2 cells post exposure to probiotic Lactobacillus acidophilus L-92, linking with immune response, DNA binding, and protein synthesis.[21] NPIPB3 was also identified to bind interferon-alpha promoter.[22] In this study, over-expression of NPIPB3 C-terminal domain reduced antagonistic activity of Type I IFN by SARS-CoV ORF6 protein (Figs. 6-8). The diacidic cluster motif (residues 53-56) was found in the ORF6 protein, as the critical determinant of subcellular localization to vesicular structures.[23] Interestingly, the C-terminal domain of NPIPB3 had several four-positively-charged-residue (KRRR) repeats. Therefore, ionic interactions could be linked with the binding interaction between SARS-CoV ORF6 and NPIPB3 C-terminal domain. In addition, the interaction between SARS-CoV ORF6 and NPIPB3 C-terminal domain might influence the binding interaction between ORF6 and karyopherin alpha 2, thus C-terminal domain of NPIPB3 recovered nuclear import carrier function of karyopherin alpha 2 in ORF6-expressing cells, correlating with STAT1 nuclear translocation post IFNβ treatment (Fig. 7). In addition, overexpression of NPIPB3 C-terminal domain reduced IFN-β-induced phosphorylation of STAT1 at Tyr701 (Fig. 8, Lane 2). Tyrosine-protein kinase JAK1 contained a putative phosphoinositide binding site; an interaction between JAK1 and PI-3-kinase was reported in IL-2 signaling pathway.[24]

Meanwhile, NPIPB3, also known as PI-3-kinase-related kinase SMG-1, showed functional and structural similarities to PI-3-kinase.[25] Therefore, NPIPB3 overexpression might increase the interaction with JAK1, in which influenced IFN-β-induced JAK/STAT signaling, resulting in the decrease of STAT1 phosphorylation at Tyr701.

In conclusion, SARS-CoV ORF6-interacting proteins including CCNL1, RBMXL2, NPIPB3, and karyopherin alpha 2 were involved in RNA splicing, nuclear pore complex formation, as well as nuclear export and import of some transcription and splicing factors. This study demonstrated SARS-CoV ORF6 inhibiting IFNβ-induced ISRE promoter, STAT1 nuclear translocation and phosphorylation. In contrast, the interaction of SARS-CoV ORF6 with C-terminal domain of NPIPB3 in human promonocytes reduced Type I IFN antagonism of ORF6.

Conflicts of interest

All authors have no conflicts of interest to declare.

Acknowledgment

We would like to thank the Ministry of Science and Technology (Taiwan) and China Medical University for financial support (CMU103-S-04, CMU101-ASIA-05, and CMU102-ASIA-15), and the Ministry of Science and Technology (MOST101-2320-B-039-036-MY3, and MOST102-2320-B-039-044-MY3).

References

1. Drosten C, Günther S, Preiser W, van der Werf S, Brodt HR, Becker S, et al. Identification of a novel coronavirus in patients with severe acute respiratory syndrome. *N Engl J Med* 2003; 348:1967-76.

2. Marra MA, Jones SJ, Astell CR, Holt RA, Brooks-Wilson A, Butterfield YS, et al. The Genome sequence of the SARS-associated coronavirus. *Science* 2003; 300:1399-404.

3. Tan YJ, Lim SG, Hong W. Characterization of viral proteins encoded by the SARS-coronavirus genome. *Antiviral Res* 2005; 65:69-78.

4. Narayanan K, Huang C, Makino S. SARS coronavirus accessory proteins. *Virus Res* 2008; 133: 113-21.

5. Liu DX, Fung TS, Chong KK, Shukla A, Hilgenfeld R. Accessory proteins of SARS-CoV and other coronaviruses. *Antiviral Res* 2014; 109:97-109.

6. Frieman M, Yount B, Heise M, Kopecky-Bromberg SA, Palese P, Baric RS. SARS-CoV ORF6 antagonizes STAT1 function by sequestering nuclear import factors on the rER/Golgi membrane. *J Virol* 2007; 81:9812-24.

7. Ye Z, Wong CK, Li P, Xie Y. A SARS-CoV protein, ORF-6, induces caspase-3 mediated, ER stress and JNK-dependent apoptosis. *Biochim Biophys Acta* 2008; 1780:1383-7.

8. Yount B, Roberts RS, Sims AC, Deming D, Frieman MB, Sparks J, et al. Severe acute respiratory syndrome coronavirus group-specific open reading frames encode nonessential functions for replication in cell cultures and mice. *J Virol* 2005; 79:14909-22.

9. Kopecky-Bromberg SA, Martínez-Sobrido L, Frieman M, Baric RA, Palese P. Severe acute respiratory syndrome coronavirus open reading frame (ORF) 3b, ORF 6, and nucleocapsid proteins function as interferon antagonists. J Virol 2007; 81:548-57.

10. Lin CW, Lin KH, Lyu PC, Chen WJ. Japanese encephalitis virus NS2B-NS3 protease binding to phage-displayed human brain proteins with the domain of trypsin inhibitor and basic region leucine zipper. *Virus Res* 2006; 116:106-13.

11. Lin CW, Cheng CW, Yang TC, Li SW, Cheng MH, Wan L, et al. Interferon antagonist function of Japanese encephalitis virus NS4A and its interaction with DEAD-box RNA helicase DDX42. *Virus Res* 2008; 137:49-55.

12. Lin YJ, Chang YC, Hsiao NW, Hsieh JL, Wang CY, Kung SH, et al. Fisetin and rutin as 3C protease inhibitors of enterovirus A71. *J Virol Methods* 2012; 182:93-8.

13. Li SW, Lai CC, Ping JF, Tsai FJ, Wan L, Lin YJ, et al. Severe acute respiratory syndrome coronavirus papain-like protease suppressed alpha interferon-induced responses through downregulation of extracellular signal-regulated kinase 1-mediated signalling pathways. *J Gen Virol* 2011; 92:1127-40.

14. Yang TC, Li SW, Lai CC, Lu KZ, Chiu MT, Hsieh TH, et al. Proteomic analysis for Type I interferon antagonism of Japanese encephalitis virus NS5 protein. *Proteomics* 2013; 13:3442-56.

15. Hussain S, Gallagher T. SARS-coronavirus protein 6 conformations required to impede protein import into the nucleus. *Virus Res* 2010; 153:299-304

16. Sims AC, Tilton SC, Menachery VD, Gralinski LE, Schäfer A, Matzke MM, et al. Release of severe acute respiratory syndrome coronavirus nuclear import block enhances host transcription in human lung cells. *J Virol* 2013; 87:3885-902.

17. Dickinson LA, Edgar AJ, Ehley J, Gottesfeld JM. Cyclin L is an RS domain protein involved in pre-mRNA splicing. J Biol Chem 2002; 277:25465-73.

18. Graveley BR. Sorting out the complexity of SR protein functions. *RNA* 2000; 6:1197-211.

19. Elliott DJ, Venables JP, Newton CS, Lawson D, Boyle S, Eperon IC, et al. An evolutionarily conserved germ cell-specific hnRNP is encoded by a retrotransposed gene. *Hum Mol Genet* 2000; 9:2117-24.

20. Martin J, Han C, Gordon LA, Terry A, Prabhakar S, She X, et al. The sequence and analysis of duplication-rich human chromosome 16. *Nature* 2004; 432:988-94.

21. Yanagihara S, Fukuda S, Ohno H, Yamamoto N. Exposure to probiotic Lactobacillus acidophilus L-92 modulates gene expression profiles of epithelial Caco-2 cells. *J Med Food* 2012; 15:511-9.

22. Qu JH, Cheng J, Zhang LX, Zhong YW, Liu Y, Wang L, et al. Screening of binding proteins to interferon-alpha promoter DNA by phage display technique. *Zhonghua Gan Zang Bing Za Zhi* 2005; 13:520-3.

23. Gunalan V, Mirazimi A, Tan YJ. A putative diacidic motif in the SARS-CoV ORF6 protein influences its subcellular localization and suppression of expression of co-transfected expression constructs. *BMC Res Notes* 2011; 4:446.

24. Migone TS, Rodig S, Cacalano NA, Berg M, Schreiber RD, Leonard WJ. Functional cooperation of the interleukin-2 receptor beta chain and Jak1 in phosphatidylinositol 3-kinase recruitment and phosphorylation. *Mol Cell Biol* 1998; 18:6416-22.

25. Baretić D0, Williams RL. PIKKs--the solenoid nest where partners and kinases meet. *Curr Opin Struct Biol* 2014; 29:134-42.

Figure legends

Fig. 1. Expression and purification of *E. coli*-synthesized SARS-CoV ORF6 protein. ORF6 gene was amplified using PCR and cloned into pTriEx™-4 Neo vector (A). ORF6-His tagged proteins were synthesized in transformed *E. coli* BL21 (DE3), purified using immobilized-metal affinity chromatography, separated using SDS-PAGE, and then examined using Western blotting with anti-His tag (B).

Fig. 2. Biopanning of phage-display a human lung cDNA library with ORF6-His tagged protein. After fifth round of biopanning with ORF6, each phage clone was randomly picked up from individual plaques, amplified in *E. coli*, and performed using direct binding ELISA with ORF6-coated plates and anti-phage antibodies. **p* value < 0.05; ***p* value < 0.01; ****p* value < 0.001 by Scheffe's test.

Fig. 3. Direct binding ELISA of high affinity phage clones to ORF6-His tagged protein. High affinity phage clone was amplified in *E. coli*, quantitated using plaque assay, and then performed by direct binding ELISA with ORF6-coated plates and anti-phage antibodies. **p* value < 0.05; ***p* value < 0.01; ****p* value < 0.001 by Scheffe's test.

Fig. 4. Co-immunoprecipitation of ORF6-His tagged protein with Trx-NPIPB3 fusion protein. Purified ORF6-His tagged protein mixed with Trx-NPIPB3 fusion protein was incubated with anti-Trx antibodies at 4^{o}C overnight, followed by incubation with protein A-Sepharose beads for a further 2 h. After centrifugation, the pellet was washed with NET buffer, samples were analysed by SDS-PAGE,

western blotting and immunoanalysis using rabbit anti-Trx and mouse anti-His tag antibodies.

Fig. 5. Colocalization analysis of SARS-CoV ORF6 and C-terminal domain of NPIPB3 in human promonocytes using confocal microscopy. Transfected cells with single or both of pTriEx-ORF6 and pDsRed-NPIPB3 were fixed, and stained with anti-His tag, followed by FITC-conjugated anti-mouse IgG antibodies, and then analyzed by confocal microscopy.

Fig. 6. The effect of NPIPB3 overexpression on the activity of the ISRE-based *cis*-reporter. Cells were transiently co-transfected with single or both of pTriEx-ORF6 and pDsRed-NPIPB3, plus control and ISRE luciferase reporters. Firefly and renilla luciferase enzymes were measured 4 h post IFNβ treatment. According to the dual Luciferase Reporter Assay System, the relative firefly luciferase activity was normalized by renilla luciferase. *p value < 0.05; **p value < 0.01; ***p value < 0.001 by Scheffe's test.

Fig. 7. Effect of NPIPB3 overexpression on IFNβ-induced nuclear translocation of STAT1 in vector control and ORF6-expressing cells. Mock (A) and IFNβ-treated (B) cells transfected with single or both of pTriEx-ORF6 and pDsRed-NPIPB3 were fixed, and reacted with anti-STAT1 and FITC-conjugated anti-mouse IgG antibodies. Finally, cells were stained with DAPI for 10 minutes, imaging analyzed by confocal microscopy.

Fig. 8. Effect of NPIPB3 overexpression on IFNβ-induced STAT1

Phosphorylation at Tyr701 in vector control and ORF6-expressing cells using Western blotting. Cells were transiently transfected with single or both of pTriEx-ORF6 and pDsRed-NPIPB3, and then treated with IFNβ. After 0-, 15- and 30-min treatment, the lysate was analyzed by Western blotting with anti-phosphotyrosine STAT1 (Tyr701), and anti-β-actin antibodies. The immune complexes were visualized using horseradish peroxidase-conjugated goat anti-mouse IgG antibodies and enhanced chemiluminescence.

Fig. 1

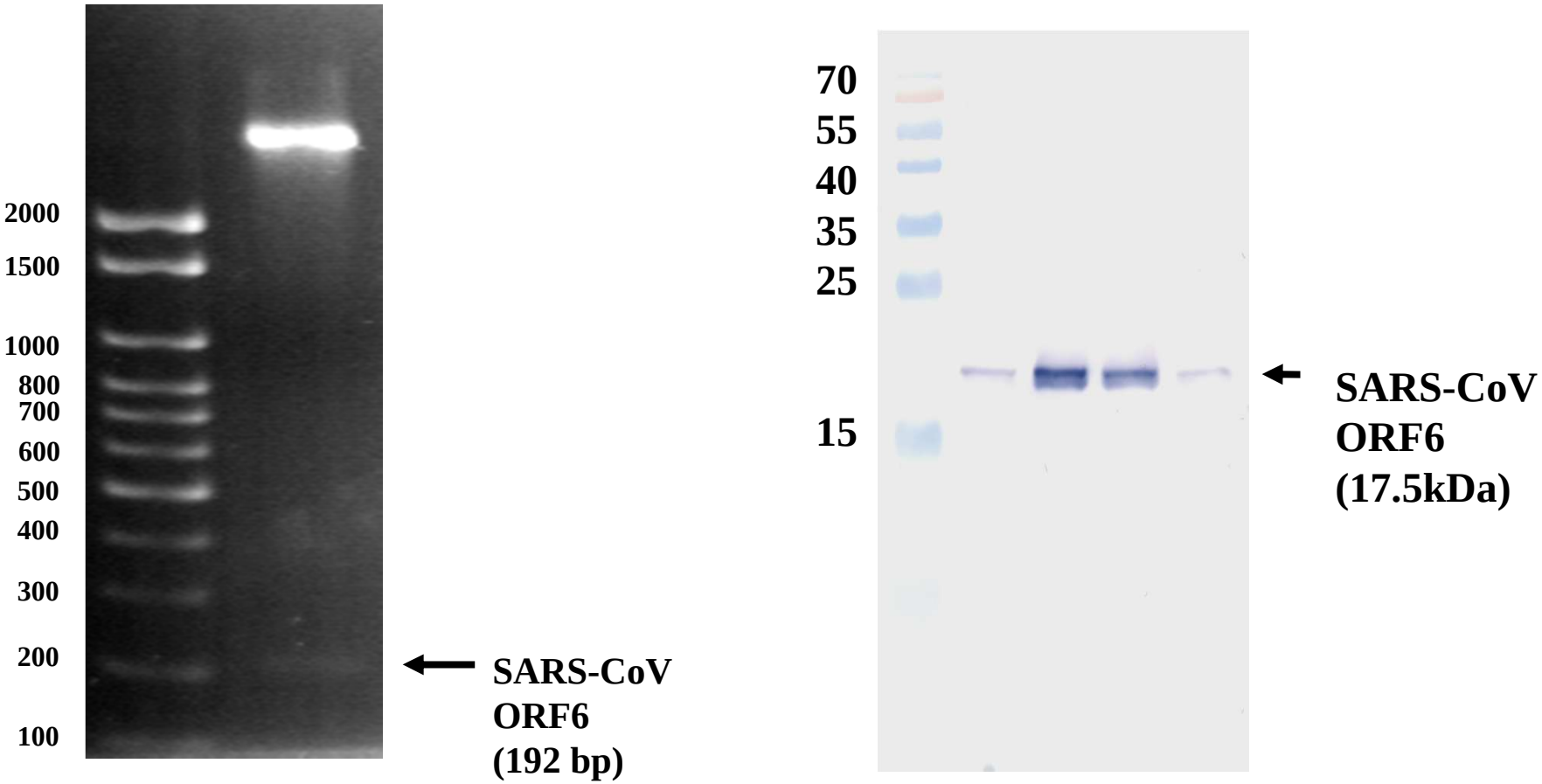

Fig. 2

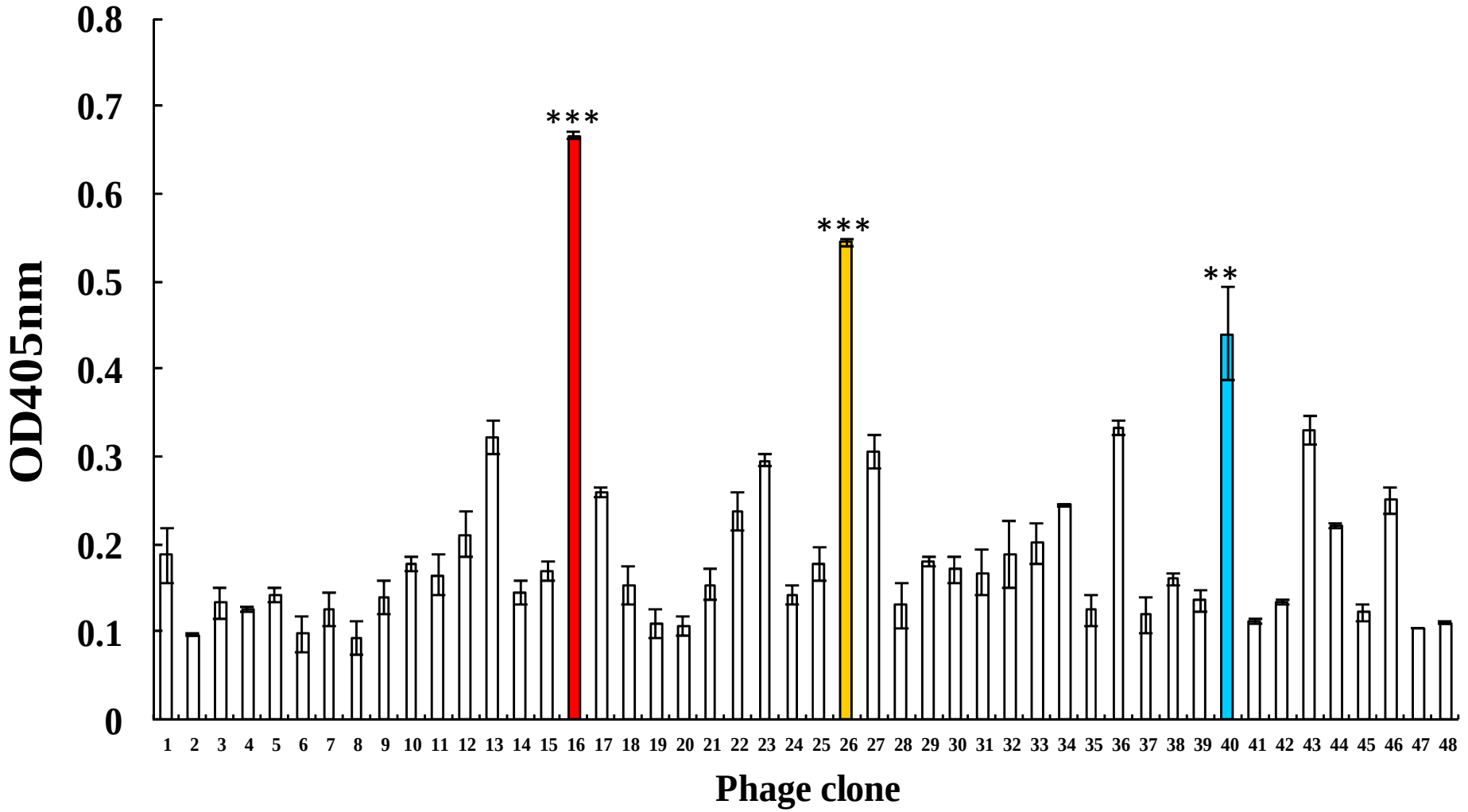

Fig. 3

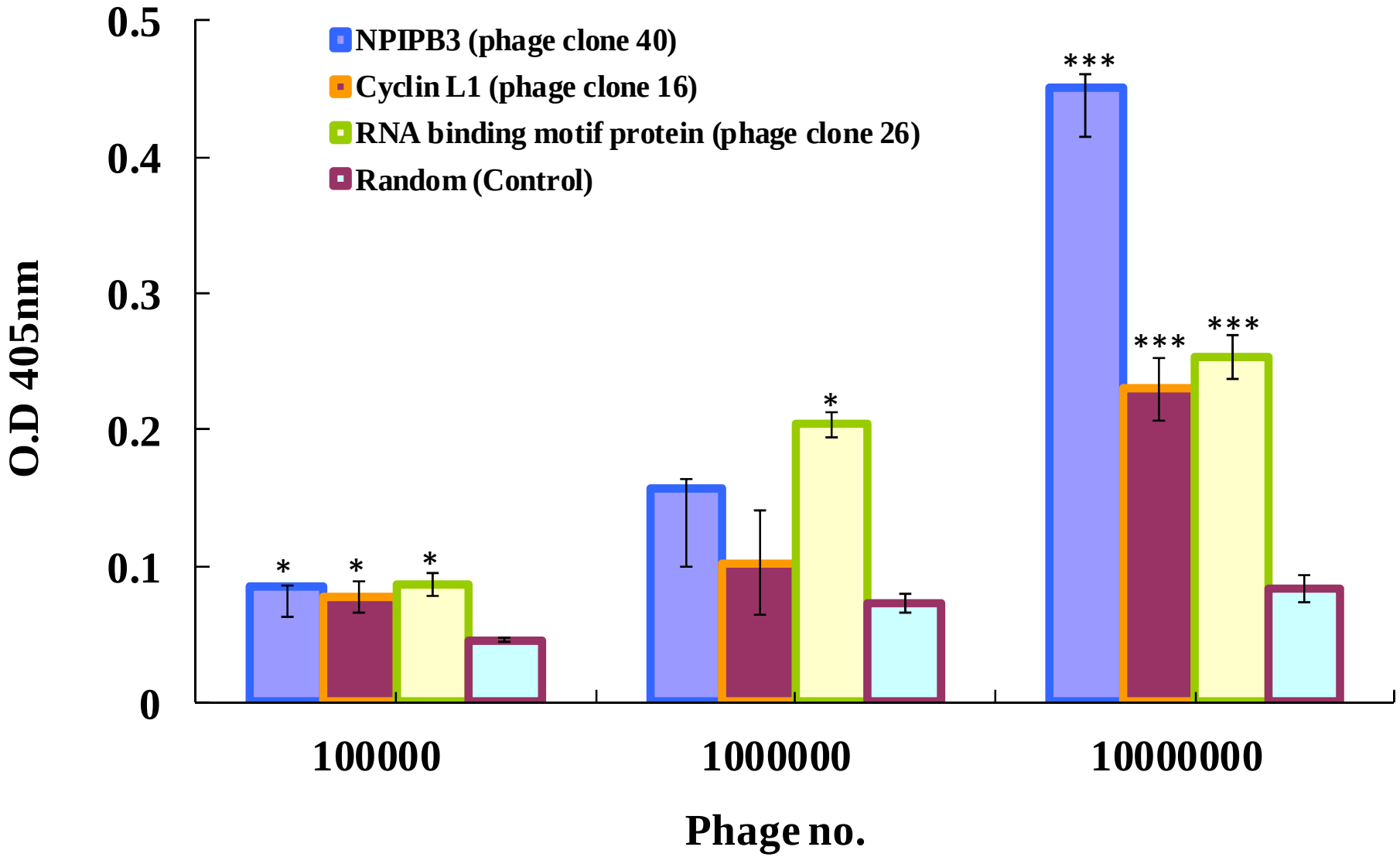

Fig. 4

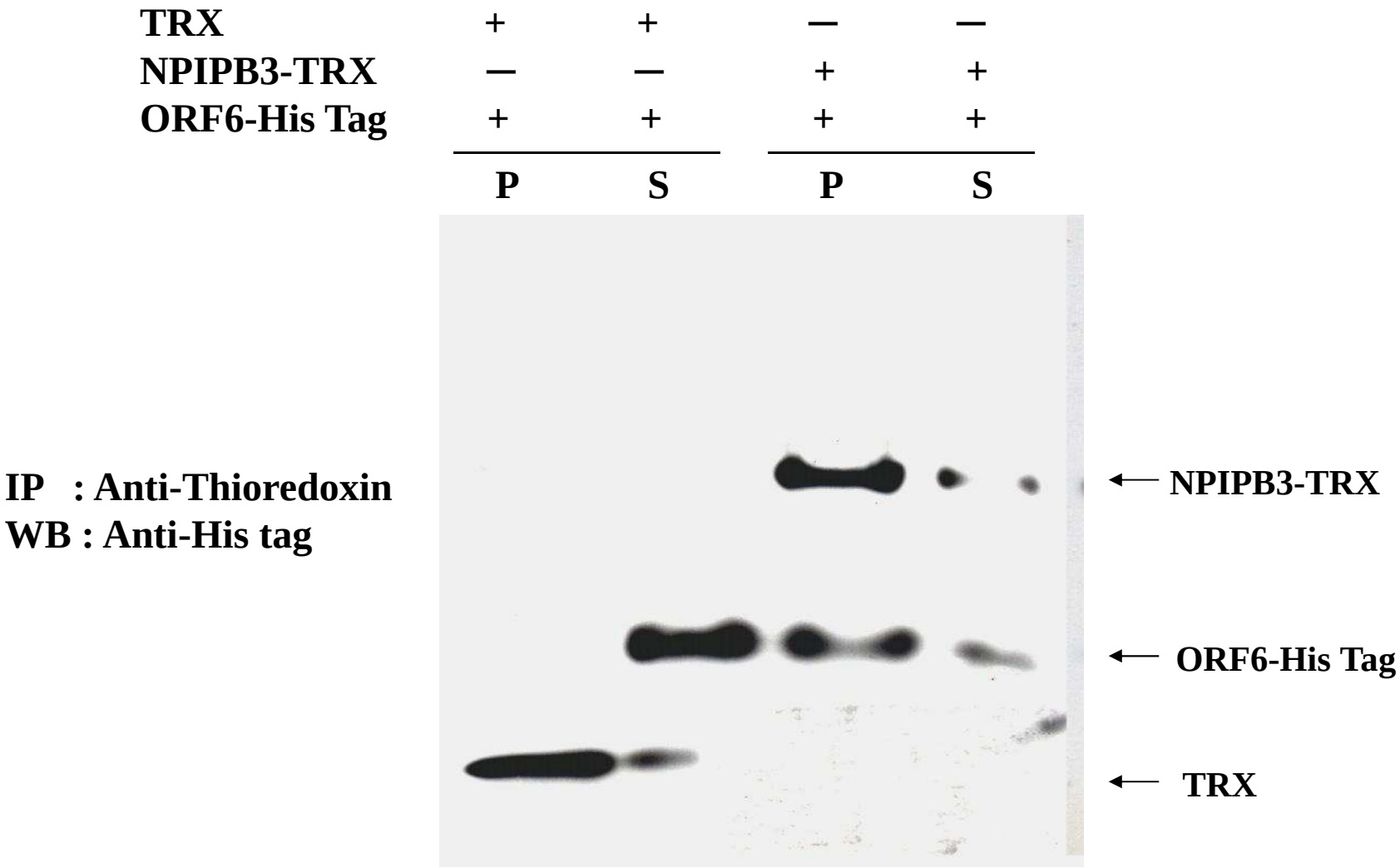

Fig. 5

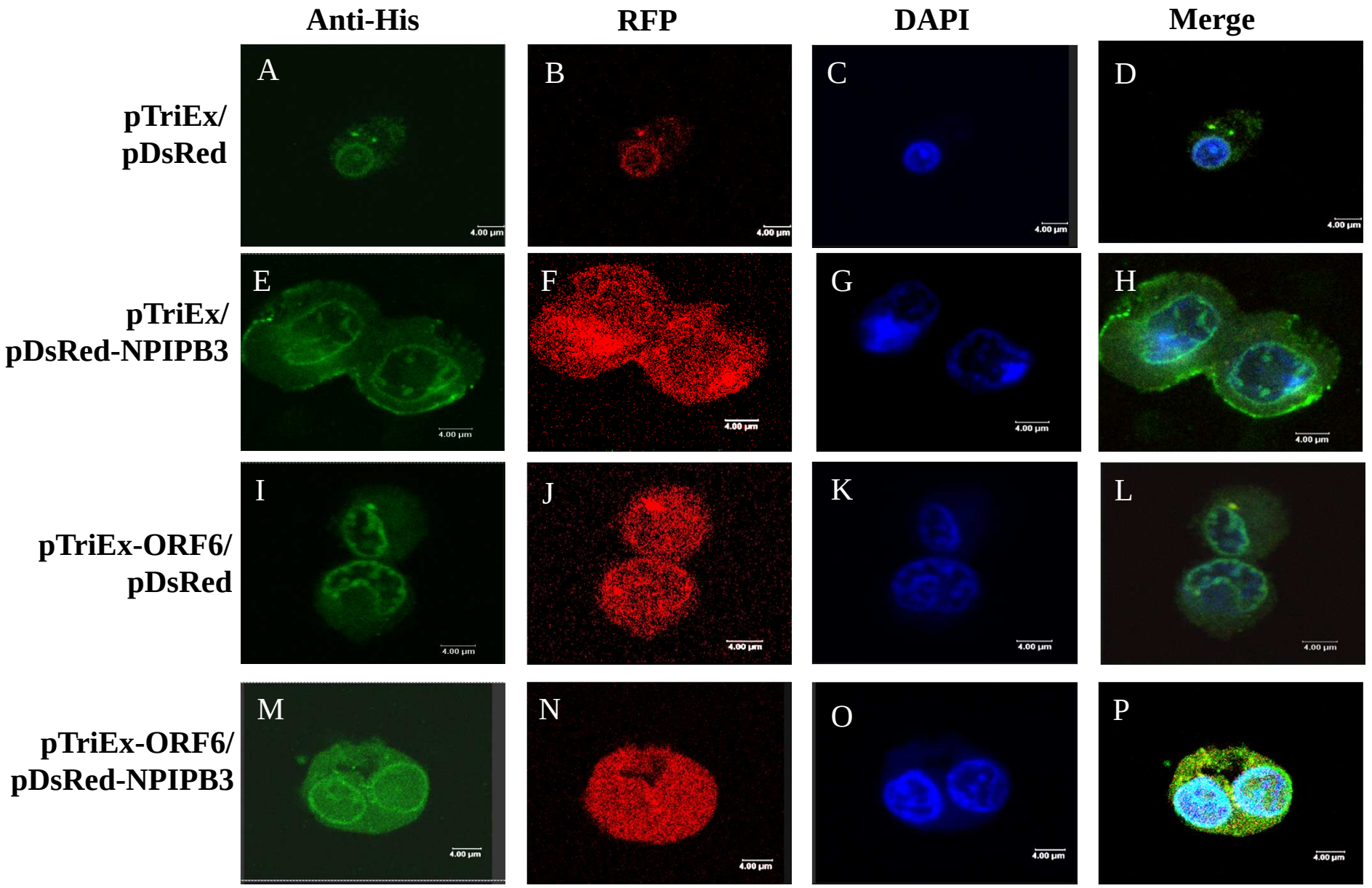
Anti-His
RFP
DAPI
Merge
pTriEx/ pDsRed
pTriEx/ pDsRed-NPIPB3
pTriEx-ORF6/ pDsRed
pTriEx-ORF6/ pDsRed-NPIPB3
A
B
C
D
E
F
G
H
I
J
K
L
M
N
O
P
4.00 µm

Fig. 6

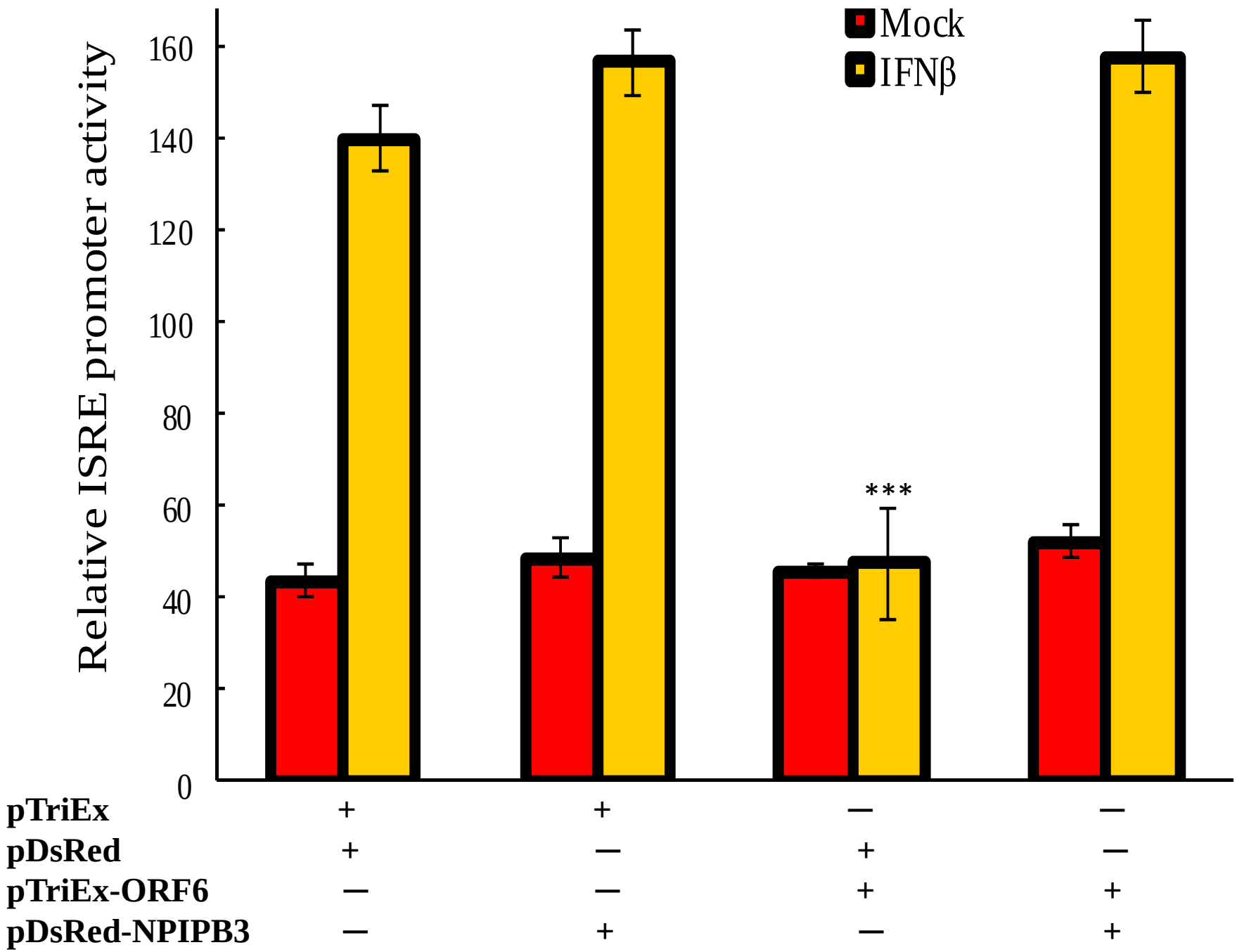

Fig. 7A

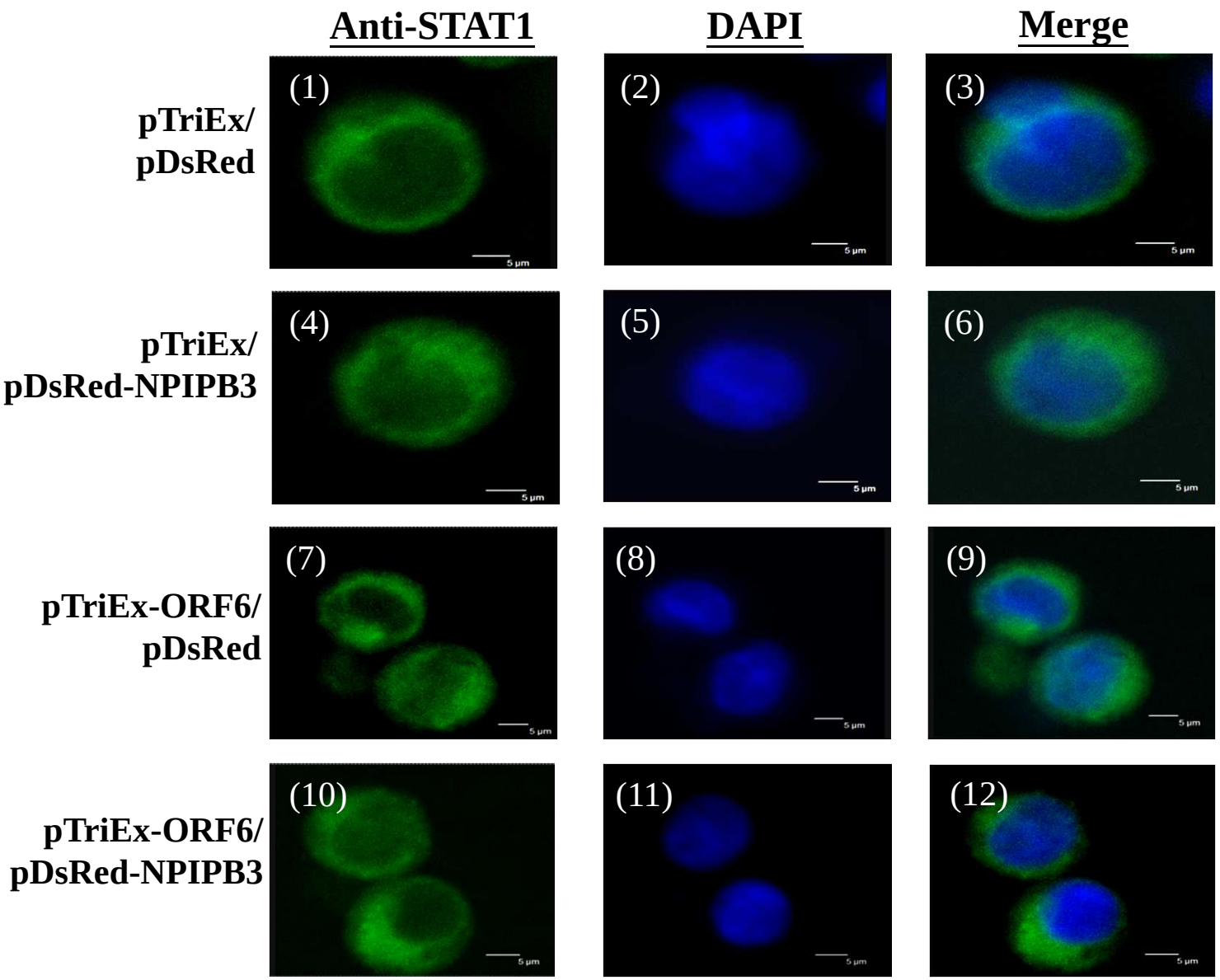
Anti-STAT1
DAPI
Merge
pTriEx/ pDsRed
pTriEx/ pDsRed-NPIPB3
pTriEx-ORF6/ pDsRed
pTriEx-ORF6/ pDsRed-NPIPB3
(1)
(2)
(3)
(4)
(5)
(6)
(7)
(8)
(9)
(10)
(11)
(12)
5 μm

Fig. 7B

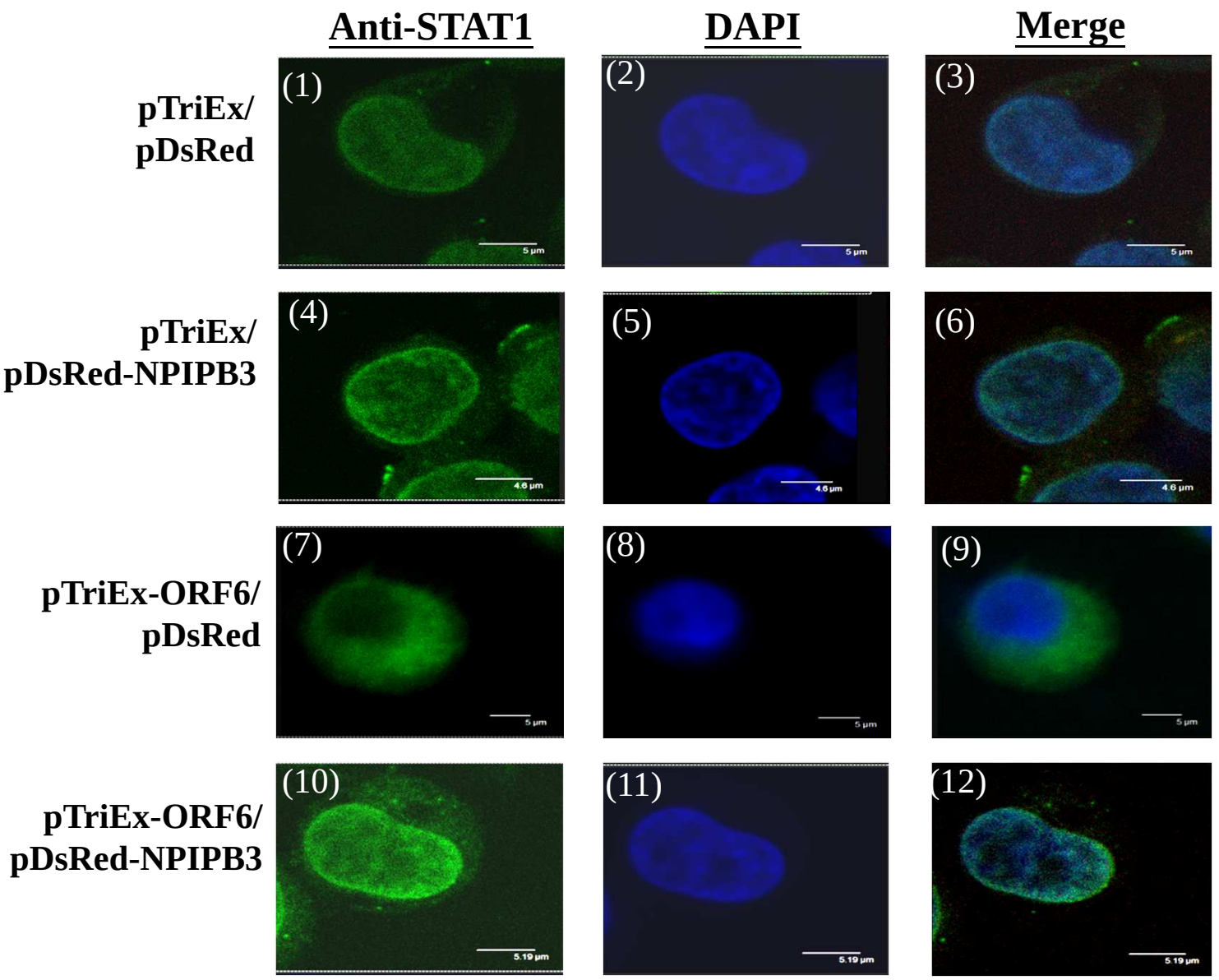
Anti-STAT1
DAPI
Merge
pTriEx/ pDsRed
pTriEx/ pDsRed-NPIPB3
pTriEx-ORF6/ pDsRed
pTriEx-ORF6/ pDsRed-NPIPB3
(1)
(2)
(3)
(4)
(5)
(6)
(7)
(8)
(9)
(10)
(11)
(12)
5 μm
4.6 μm
5.19 μm

Fig. 8